FERMILAB-PUB-75-165-E #188 PRL

Inclusive Cross Sections for p + n → p + X Between 50 and 400 GeV*

B. Robinson†, K. Abe, J. Carr, J. Keyne,
A. Pagnamenta, F. Sannes, I. Siotis and R. Stanek

Rutgers University, New Brunswick, N. J. 08903,
Imperial College, London SW7, U.K.
and University of Illinois,
Chicago, Ill. 60680

ABSTRACT

We have measured the inclusive cross sections for the reaction $p + d \to p + X$ in the region $0.14 < |t| < 0.38$ GeV^2, $100 < s < 750$ GeV^2 and $0.80 < x < 0.93$ using the acceleration ramp and deuterium gas jet target at Fermilab. These measurements are combined with our earlier measurements of $p + p \to p + X$ to obtain invariant cross sections for $p + n \to p + X$.

*Research supported by the U. S. National Science Foundation and the Science Research Council, U. K. Development and operation of hydrogen jet target supported by the State Committee for Utilization of Atomic Energy of the U. S. S. R., Moscow.

†Present Address: University of Washington
Seattle, Washington 98105

In a recent experiment we have measured the inclusive cross sections for the reactions

$$p + p \rightarrow p + X \quad (1 + 2 \rightarrow 3 + X) \qquad (1)$$

$$p + d \rightarrow p + X \quad (1 + 2 \rightarrow 3 + X) \qquad (2)$$

using the hydrogen and deuterium gas jet targets in the Fermilab main ring. The results of the $pp \rightarrow pX$ measurements were reported earlier.[1] In this letter we present cross sections for the reaction $pd \rightarrow pX$ and combine the two sets of measurements to obtain invariant cross sections for the reaction

$$p + n \rightarrow p + X \quad (1 + 2 \rightarrow 3 + X) \qquad (3)$$

The variables we use are

$$s = m_1^2 + m_2^2 + 2E_1 m_2 \qquad (4)$$

$$t = m_2^2 + m_3^2 - 2E_3 m_2 \qquad (5)$$

$$x \equiv 1 - M_X^2/s = (2E_1E_3 - 2p_1p_3 \cos \theta_3 + 2E_3m_2 - m_3^2)/s \qquad (6)$$

where s, t and M_X^2 are the squares of the total center-of-mass energy, the four-momentum transfer and the mass of X respectively and θ_3 is the laboratory recoil angle of particle 3. Since we wish to compare our pd data to our pp data, it is convenient to use the nucleon rather than the deuteron mass for m_2 in Eqs. (4-6) to describe Reaction (2), i.e., we assume independent nucleon-nucleon interactions, the second nucleon in the deuteron being a spectator.

The recoil particles were detected and identified as protons in a spectrometer consisting of a series of scintillation counters as described in Ref. 1. In addition, we detected elastically scattered deuterons in a small solid state detector at 85.5^{o} from the beam direction. The beam-target luminosity was determined as in Ref. 1 using the pd elastic differential cross sections of Akimov et al.[2] and the total pd cross sections of Carroll et al.[3]

The pd $\rightarrow$ pX data are shown in Fig. 1. Only statistical errors to which we have added quadratically systematic errors of ±3% are displayed. The uncertainty in the overall normalization is ±15% as for our earlier measurements[1] of pp $\rightarrow$ pX. However, since both reactions were studied with the same apparatus, the only difference being the gas used in the jet target, we estimate the relative error between the pp and pd data to be only ±4% due solely to uncertainties in the pp and pd elastic cross sections.

The cross sections for pd $\rightarrow$ pX look very similar to those for pp $\rightarrow$ pX.[1] They show a weak s dependence and an exponential t dependence of $\sim e^{6t}$. There is a minimum in the x distribution at x = 0.87 and the absolute value of the pd $\rightarrow$ pX cross section is about twice that of pp $\rightarrow$ pX. However, it should not be assumed from this similarity that the cross sections for pn $\rightarrow$ pX are the same as for pp $\rightarrow$ pX. The measured shapes of the pd inclusive spectra in our kinematic region (x near 1, low $|t|$) are determined to a large extent by the Fermi motion of the target nucleons as well as the rescattering of the recoil particle off the spectator nucleon in the deuteron.

To extract the pn $\rightarrow$ pX spectra we assume the impulse approximation. In this approximation the proton and neutron in the deuteron are considered as independent particles in close proximity.

The closeness of the nucleons gives rise to a shadowing of one by the other, effectively lowering the luminosity of both relative to an equal number of free particles. We assume the decrease in luminosity for inclusive reactions is the same as that for total cross sections, i.e., $\sigma_{pd} = \sigma_{pp} + \sigma_{pn} - \delta$ where $\delta = \sigma_{pn}\sigma_{pp}/4\pi\langle r^2\rangle$ with $\langle r^2\rangle = 31$ mb. This is the cross section deficit of Glauber theory[4] and amounts to a decrease of $\sim$5% in the effective pd cross section over our energy range.

The effect of the deuteron potential in the impulse approximation is to give the nucleons a center of mass momentum or Fermi motion. As a result of this our spectrometer will detect recoil protons originating from elastic scattering off the moving target proton. To estimate this effect we use the Hulthen wave function[5] and measured pp elastic scattering cross sections[6] in a Monte Carlo program to simulate the pp elastic spectra as seen by our spectrometer. These spectra are approximately gaussian around the elastic peak value of x which from defining Eq. (6) occurs at $x = 1 - M_p^2/s$. The same Monte Carlo program is used to smear the inelastic pp $\to$ pX spectra for which we use a composite input of all available data[7,8,9] in addition to our published measurements.[1]

For both the pp elastic and inelastic cross sections mentioned above we use the forms for "free" protons but modified by the deuteron form factor S(t) in order to exclude interactions which result in a deuteron in the final state which is not detected, i.e., for the pp differential cross sections we use $d\sigma/dt_{free}\,[1 - S^2(t)]$.

An additional feature of the Monte Carlo program is the inclusion of an estimate of the rescattering of the recoil protons by the spectator neutron which has the effect of spreading the x distributions for those protons which interact. For this we assume that the neutron on average sits at an rms radius of $\sqrt{31\ \mathrm{mb}}$ and that the reaction is the same as for free np scattering. The probability for an interaction was taken to be simply $\sigma_{pn}/4\pi\langle r^2\rangle$ and the scattering angle was weighted by low energy np differential cross section measurements.[10]

Summarizing, our final $pn \to pX$ cross sections were obtained in the following manner: 1) Our $pd \to pX$ cross sections were multiplied by 1.05 to correct for the shadowing effect. 2) From the resulting cross sections we subtracted the $pp \to pp$ elastic and $pp \to pX$ inclusive cross sections both of which were Fermi smeared, corrected for coherent pd scattering (by including the deuteron form factor) and corrected for rescattering off the spectator neutron. A typical spectrum and the distributions from which it was derived is shown in Fig. 2.

The final $pn \to pX$ spectra are plotted in Fig. 3. They contain the effects of Fermi motion and rescattering which have not been unfolded. The normalization errors have been calculated by taking into account the fact that the absolute uncertainties in the $pp \to pX$ and $pd \to pX$ data are correlated due to the use of the same apparatus for both measurements. This leads to overall normalization uncertainties for the $pn \to pX$ data of ±5.6, ±4.0, ±2.9 and ±1.8 mb/GeV^2 at $-t = 0.16$, 0.20, 0.25 and 0.33 GeV^2 respectively. The cross sections for the reaction $pn \to pX$ reported in this letter are approximately a factor three higher than those of a recent ISR measurement[11] of the reaction $pp \to nX$.

As can be seen from Fig. 3 the invariant cross section for $pn \to pX$ falls as x tends to 1 in contrast to that for $pp \to pX$ which rises above $x = 0.88$. Near $x = 0.82$ the ratio n/p of the two cross sections is about 0.8 at $-t = 0.16$ GeV^2 and 0.6 at $-t = 0.33$ GeV^2 independently of s. This implies a stronger t dependence of the cross section for $pn \to pX$ ($\sim e^{8t}$) than that of $pp \to pX$[1] ($\sim e^{6t}$). Finally, at fixed x and t the $pn \to pX$ data show no significant energy dependence although a 20% drop between the two extreme energies is possible within errors.

The study of the charge exchange reaction $pp \to nX$ (or equivalently $pn \to pX$) near $x = 1$ provides valuable information on the non-diffractive component of the reaction $pp \to pX$. The most popular phenomenological framework for discussing both reactions in our kinematic region has been the triple Regge formalism. It was first suggested by Bishari[12] that pion exchange might be the dominant mechanism for the charge exchange reaction. By extrapolating to the pion pole, Field and Fox[13] estimate the contribution of the $\pi\pi P$ and $\pi\pi R$ terms to the process $pn \to pX$. They obtain

$$G_{\pi\pi k} = \frac{1}{4\pi} \frac{g^2_{\pi np}}{4\pi} \sigma_t{}^k(\pi p) \frac{(-t)\; e^{b(t-\mu^2)}}{(t-\mu^2)^2} \qquad (7)$$

for the triple Regge couplings where k represents pomeron or reggeon exchange and $\mu^2 = m_\pi{}^2$. The total πp cross section is taken to be $\sigma_t(\pi p) = \sigma_t^P(\pi p) + \sigma_t^R(\pi p)/\sqrt{s}$ with $\sigma_t^P(\pi p) = 22$ mb and $\sigma_t^R(\pi p) = 18$ mb and the on mass shell coupling $g^2_{\pi np}/4\pi = 2\, g^2_{\pi pp}/4\pi$ is 30. For simplicity we neglect any off shell corrections by putting $b = 0$

in Eq. (7) and in the triple Regge formula[14] we use $\alpha_\pi(t) = 0.0 + t$, $\alpha_P(0) = 1$ and $\alpha_R(0) = 0.5$. Furthermore, in order to compare with the data, we modify the theoretical prediction by a Monte Carlo program to account for Fermi motion and rescattering which has the effect of raising the theoretical curves by $\sim$10% and $\sim$30% at $x = 0.82$ and 0.92 respectively. The result, which is shown in Fig. 3 for the two extreme s and t values, is in reasonable agreement with the data.

In conclusion, the results presented here strongly support the hypothesis that pion exchange plays an important role in the charge exchange reaction $pn \rightarrow pX$. The $\pi\pi P$ and $\pi\pi R$ terms should be included in any analysis of the reaction $pp \rightarrow pX$ which otherwise will overestimate the other triple Regge contributions, mainly the RRP term.

We wish to thank the members of the Internal Target Laboratory and the Accelerator Section for their help and cooperation. The advice and contributions of G. Cvijanovich, T. DeLillo, W. C. Harrison and B. Maglich are gratefully acknowledged.

References

1. K. Abe et al., Phys. Rev. Lett. 31, 1527 (1973).
2. Y. Akimov et al., Proceedings of the XVII International Conference on High Energy Physics, London, 1974.
3. A. S. Carroll et al., Fermilab Preprint No. NAL-PUB-74/75-Exp., 1974.
4. V. Franco and R. J. Glauber, Phys. Rev. 142, 1195 (1966).
5. L. Hulthen and M. Sugawara, Handbuch der Physik 39, 1 (1957).
6. G. Giacomelli, Proceedings of the XVI International Conference on High Energy Physics, Batavia, 1972, p. 219.
7. M. G. Albrow et al., II International Conference on Elementary Particles, Aix-en-Provence, 1973.
8. J. W. Chapman et al., University of Rochester Preprint No. UR-458, 1973.
9. S. J. Barish et al., Argonne National Laboratory Preprint No. ANL/HEP 7338, 1973.
10. Hadley et al., Phys. Rev. 75, 351 (1949).
11. J. Engler et al., II International Conference on Elementary Particles, Aix-en-Provence, 1973.
12. M. Bishari, Phys. Lett. 38B, 510 (1972).
13. R. D. Field and G. C. Fox, California Institute of Technology, Preprint No. CALT-68-434, 1974.
14. K. Abe et al., Phys. Rev. Lett. 31, 1530 (1973).

Figure Captions

Fig. 1 Inclusive cross sections for the reaction $pd \rightarrow pX$. The variables s, t and x are defined as if the deuterium target consisted of free protons and neutrons (see text). Errors for the two intermediate energies are similar to those shown for the two extreme energies.

Fig. 2 Sample extraction of $pn \rightarrow pX$ cross sections from $pd \rightarrow pX$, $pp \rightarrow pX$ and $pp \rightarrow pp$ cross sections at $s = 288$ GeV^2 and $t = -0.20$ GeV^2.

Fig. 3 Inclusive cross sections for the reaction $pn \rightarrow pX$. The symbols representing s = 108, 285, 503 and 752 GeV^2 are as defined in Fig. 1. The solid ($s = 108$ GeV^2) and dashed ($s = 752$ GeV^2) curves are the $\pi\pi P$ and $\pi\pi R$ contributions to the triple Regge formula. These theoretical curves have been modified to account for Fermi motion and rescattering effects which have not been unfolded from the data.

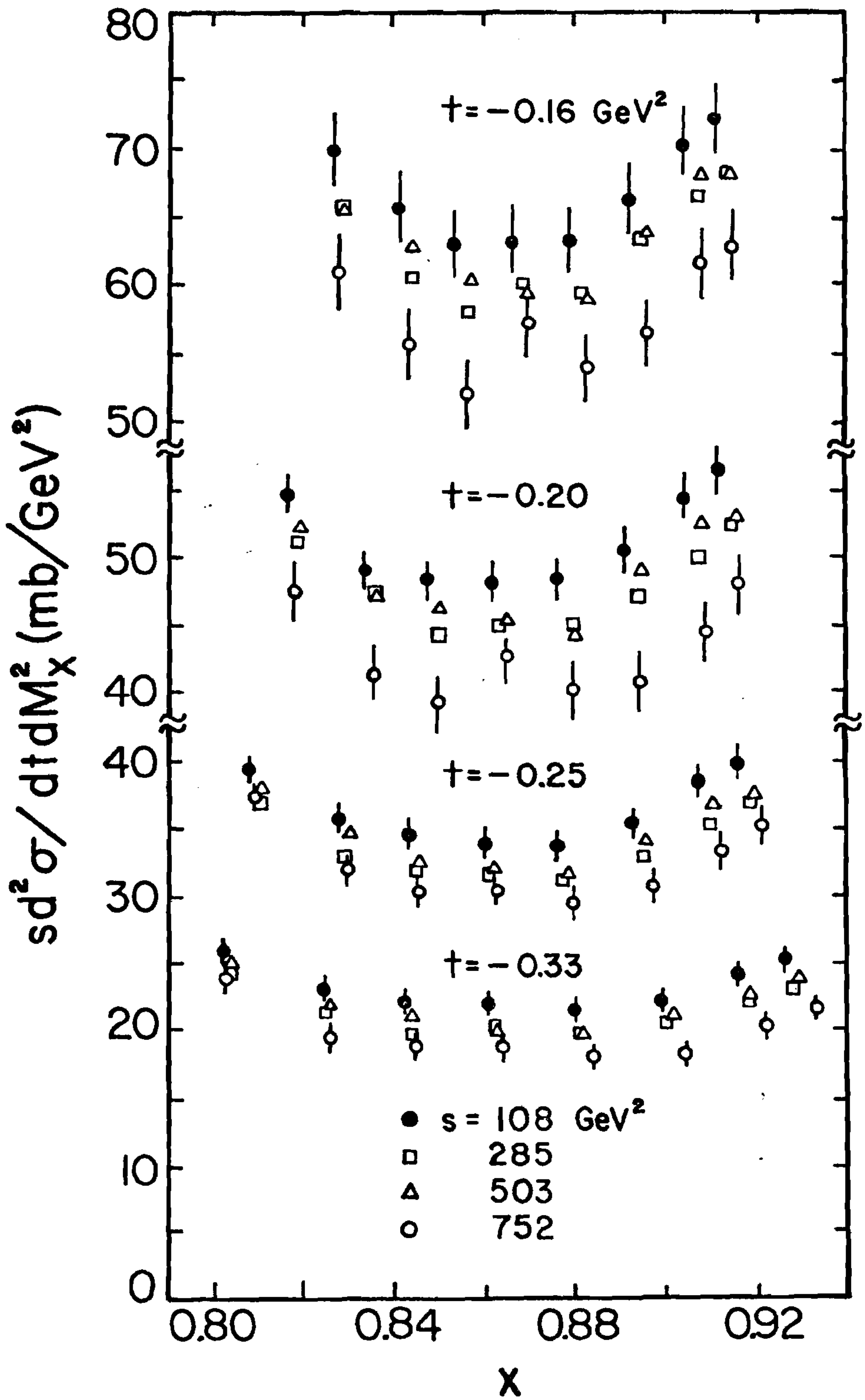

80
70
60
50
40
40
30
20
10
0
$t = -0.16\ GeV^2$
$t = -0.20$
$t = -0.25$
$t = -0.33$
$s = 108\ GeV^2$
285
503
752
$sd^2\sigma/dt\,dM_X^2\ (mb/GeV^2)$
0.80
0.84
0.88
0.92
X

Fig. 1

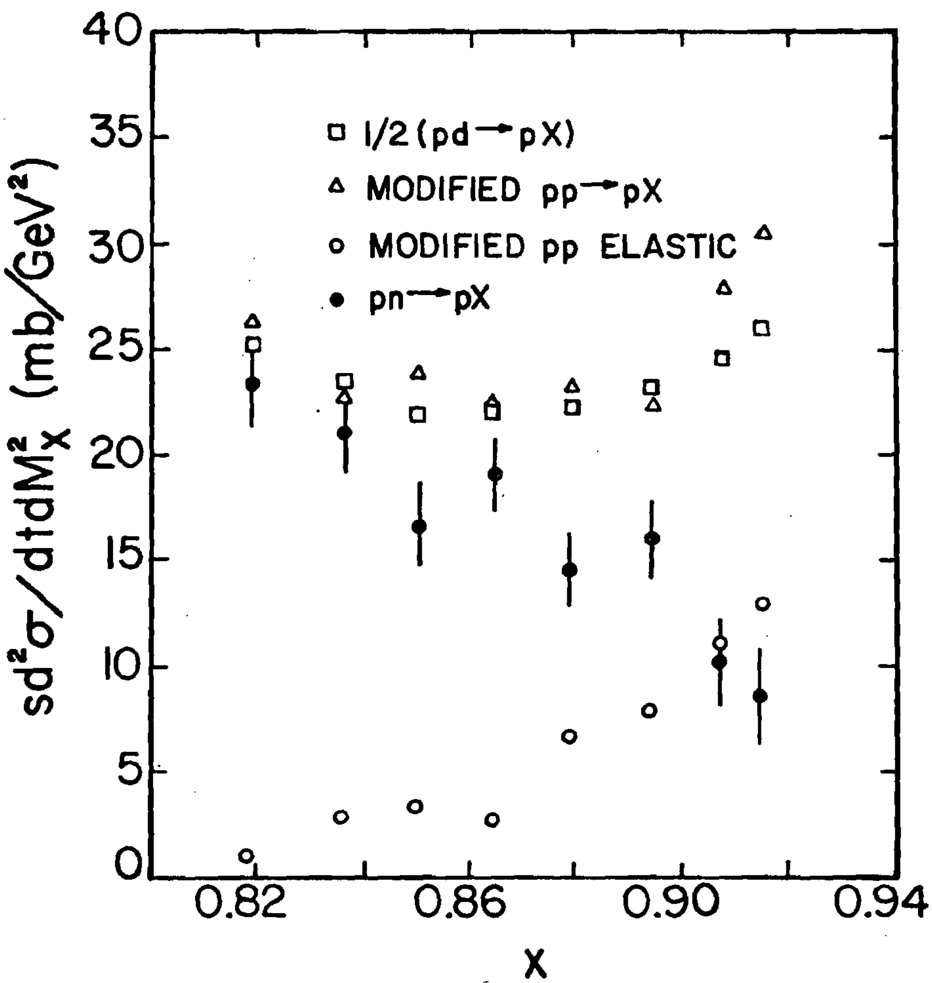

40
35
30
25
20
15
10
5
0
0.82
0.86
0.90
0.94
X
$sd^2\sigma/dtdM_X^2$ (mb/GeV^2)
□ 1/2 (pd → pX)
△ MODIFIED pp → pX
○ MODIFIED pp ELASTIC
● pn → pX

Fig. 2

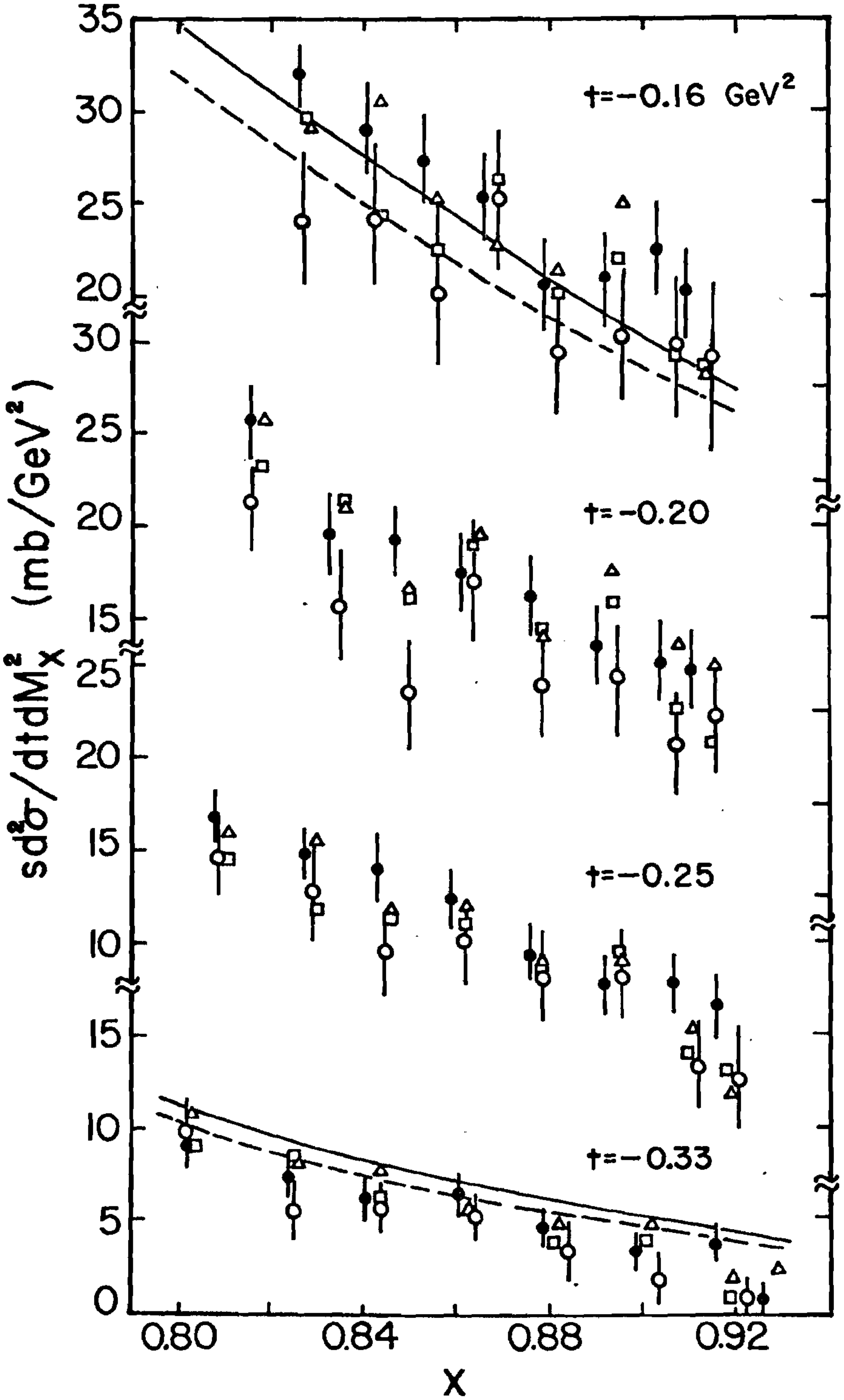

t=−0.16 GeV^2
t=−0.20
t=−0.25
t=−0.33
$sd^2\sigma/dtdM_x^2$ (mb/GeV^2)
X
0.80
0.84
0.88
0.92
35
30
25
20
15
10
5
0

Fig. 3